AIMS Materials Science, 11(4): 815–832.
DOI: 10.3934/matersci.2024040
Received: 02 July 2024
Revised: 28 August 2024
Accepted: 09 September 2024
Published: 24 September 2024

https://www.aimspress.com/journal/Materials

Research article

Characteristics of metakaolin-based geopolymers using bemban fiber additives

Nursiah Chairunnisa[1,*], Ninis Hadi Haryanti[2], Ratni Nurwidayati[1], Ade Yuniati Pratiwi[1], Yudhi Arnandha[3], Tetti N Manik[2], Suryajaya[2], Yoga Saputra[2] and Nur Hazizah[2]

[1] Civil Engineering Program, Engineering Faculty, Universitas Lambung Mangkurat, South Kalimantan, Indonesia
[2] Physics Program, Mathematics, and Natural Science Faculty, Universitas Lambung Mangkurat, South Kalimantan, Indonesia
[3] Civil Engineering Program, Engineering Faculty, Tidar University, Central Java, Indonesia

* **Correspondence:** Email: nursiah.chairunnisa@ulm.ac.id.

Abstract: The aim of this study was to investigate the chemical composition and thermal properties of kaolin, the physical properties of metakaolin, and the mechanical properties of metakaolin-based geopolymers using bemban fiber. Kaolin was calcinated to become metakaolin at 600 °C for 2 h for optimum conditions. The chemical composition of kaolin mostly consisted of 59.30% SiO_2, 34.30% Al_2O_3, and 3.06% Fe_2O_3. The transformation of kaolin into metakaolin with temperature was determined through thermal stability tests and analyzed using thermogravimetric analysis (TGA) and differential thermal analysis (DTA). Regarding the thermal properties of kaolin, predehydroxylation occurred at 31.07–92.69 °C, dihydroxylation occurred at 400–600 °C, and the endothermic peak in the DTA curve was recorded at 505.63 °C. This research also analyzed the physical and mechanical characteristics of metakaolin-based geopolymers, with the additional variation percentages of bemban fiber alloys resulting from a 3% NaOH alkalization treatment for 2 h. The test results indicate that the bemban fiber improves the physical and mechanical characteristics of geopolymers. This improvement is related to the enhanced geopolymer characteristics, including a water absorption capacity of 1.10%, porosity of 2.32%, compressive strength of 35.33 MPa, and splitting tensile strength of 11.29 MPa with the addition of 1.5% bemban fiber. Although the split tensile strength increases as the fiber content increases, adding 1.5% of bemban fiber is optimum because a higher content decreases the workability of mixtures.

Keywords: geopolymer mortars; bemban fiber; metakaolin; porosity; compressive strength

1. Introduction

The need for environment-friendly construction and industrial materials has encouraged the development of geopolymer production using natural fibers. The benefits of using natural fibers include biodegradability, renewability, relatively high specific strength properties, reduced wear (not being too abrasive to the processing equipment), low cost, and abundance in nature [1]. Geopolymers are increasingly in demand because they can be produced from inorganic aluminosilicate materials such as metakaolin and industrial waste such as fly ash. Geopolymers are synthesized from aluminosilicate-based sources and alkali activators mixed with water for various applications [2]. In this context, natural fibers are used as an alternative to develop geopolymers.

Compared to normal concrete, which uses 100% Portland cement, geopolymers have several advantages, especially in improving environmental sustainability. Geopolymers do not use Portland cement or zero cement, being called green concrete [3,4]. Geopolymers use 100% waste materials such as fly ash, slag, rice husk ash, palm shell ash, and others as raw material cement substitutes. Hence, geopolymers minimize CO_2 emissions by up to 80% compared to the Portland cement production process, which produces 5%–7% of the world's CO_2 emissions [3,5]. In the meantime, the primary source of energy and CO_2 emissions from geopolymers is the activating solution [3]. In addition to their positive effects on the environment, geopolymers are mechanically superior to normal concrete [6,7]. These materials are also more durable, showing less shrinking. Geopolymers have good thermal stability, chemical resistance, and long-term durability, making them ideal for a variety of uses in building and transportation and even as fire-resistant materials [8–12].

The main weakness of the natural fibers used in geopolymers is the high lignin-hemicellulose content, resulting in low resistance to water absorption, low dimensional stability, and low adhesive properties. Currently, there are methods to improve the performance and compatibility of natural fibers with a geopolymer matrix, by modifying the fiber surface with alkalization. Sá Ribeiro et al. [13] reported an increase in tensile strength in metakaolin-based geopolymers reinforced with alkalized bamboo fibers compared to untreated ones, explaining that these fibers in a geopolymer matrix showed increased interfacial bonding (adhesiveness). Besides these fibers, bemban fiber (*Donax canniformis*) can also be used in geopolymers.

Bemban is a potential natural resource in South Kalimantan, growing wild in swamp areas with an acidic peat soil structure [14]. Bemban is often found on the banks of water, in wet places, or in wild bamboo forests. Normally, people use bemban fibers to tie the roofs of animal cages made from dry sago leaves and bamboo [15]. Saputra et al. [16] also explored the use of bemban fiber as an additional material for porous asphalt. The use of bemban fiber as a geopolymer alloy material is the most recent application, especially as the fiber has beneficial properties such as high durability and resistance to solar heat, cold weather, wear and tear, and rotting [17].

A variety of materials, such as clay and industrial wastes like slag, ash, and waste glass, can be used to make geopolymers [18–21]. Kaolinite can be defined as the first and main component for creating geopolymers [22]. After being effectively employed, scientists started to develop it by calcining the kaolinite clay to produce metakaolin [23]. As a raw material for geopolymer, metakaolin (MK) is anticipated to gain more appeal and practicality in the future due to its substantial SiO_2 and Al_2O_3

content and more stable chemical composition than those waste materials [23–26]. Besides biological resources like bemban plants, South Kalimantan also has abundant mineral wealth, including kaolin, which is spread across several districts, amounting to more than 31 million tons (South Kalimantan PMPTSP Service, 2022) out of the total 1.154 million tons of kaolin in Indonesia, with a production volume of 629,247 m^3 in 2020 (Central Statistics Agency, 2020). Kaolin is a rock mass composed of clay or clay material, which is white or slightly whitish [27]. According to Saukani et al. [8], to obtain kaolin with high amorphousness and perfect metakaolin formation, it should be calcined for 3 h at a temperature of 750 °C. The chemical composition of kaolin includes 44.17%–46.15% SiO_2 and 36.55%–49.91% Al_2O_3, which are potential materials for creating geopolymers [28].

This research uses metakaolin and bemban fiber (*D. canniformis*) as geopolymer materials. Fiber alkalization treatment used 3% NaOH for 2 h and kaolin calcination for 2 h at varying temperatures from 550 to 800 °C. Geopolymer characteristics are investigated in terms of physical and mechanical properties. Previous research showed significant results for the behavior of metakaolin-based concrete geopolymers [24,29,30]. The expected benefit is that the load fiber can improve the characteristics of the geopolymer, which is useful in the production of environmentally friendly construction and industrial materials.

2. Materials and methods

2.1. Material

The basic materials of geopolymer mortars used include metakaolin and silica sand as fine aggregate with characteristics of 5% sludge content, organic content (color 3), and zone 4 sieve analysis. NaOH (8M) and Na_2SiO_3 are used as activators in a ratio of 2.5:1. The mortar produced consists of 65% fine aggregate and 35% paste, while the paste contains 60% fly ash or metakaolin and 40% alkaline solution. Bemban fiber is used as an additive in the mortar mixture to improve geopolymer performance.

2.1.1. Inspection analysis of kaolin clay

The kaolin material was obtained from Kupang Mountain, Banjarbaru City, South Kalimantan Province, Indonesia. The kaolin analysis comprised X-ray fluorescence (XRF) analysis to obtain the chemical composition of kaolin and the physical properties of metakaolin such as density, porosity, and water content. The thermal properties of kaolin and metakaolin were also analyzed.

Kaolin, applied as a geopolymer material, is hydroxylated to become metakaolin. The transformation of kaolin into metakaolin, with temperature and holding time, was determined through thermal stability tests using differential thermal analysis (DTA) and thermogravimetric analysis (TGA). The kaolin was washed to separate it from other impurities and then dried using an oven at a temperature of 105 ± 5 °C for 24 h. Thereafter, it was ground and filtered through a 200-mesh sieve and calcined using a furnace at varying temperatures of 550, 600, 650, 700, 750, and 800 °C for 2 h. The identification of functional groups in kaolin and metakaolin was carried out through Fourier-transform infrared spectroscopy (FTIR) analysis with a wave number range of 4000–500 cm^{-1}.

2.1.2. Alkalization of bemban fiber

The bemban fiber used in this study was sourced from bemban plants in Kanamit Village, Pulang Pisau Regency. The bemban stems were cleaned and cut to a size of ± 20 cm and boiled for ± 60 min. The fibers were then combed longitudinally to obtain the bemban fiber and dried in an oven at 75 °C for ± 4 h [15]. Bemban fiber was prepared with alkalization treatment using 3% NaOH for 2 h, before being applied as a constituent material of geopolymer as an additive.

2.1.3. Silica sand as fine aggregate

Silica sand was taken from Panggung Village, Pelaihari, South Kalimantan. The silica sand characterization was tested for water content using SNI 03-1971-1990, the sludge content was based on SNI S-04-1989-F, the organic content was based on SNI 2816-2014, and sieve analysis was based on ASTM C136:2012.

2.2. Method

The study used 100% metakaolin as the raw material for the geopolymer**.** An alkaline solution was mixed with metakaolin powder to prepare the geopolymer mortar. Metakaolin-based geopolymer specimens consisting of NaOH (8M) and Na_2SiO_3 were used as activators in a ratio of 2.5:1.

The chemical composition and thermal properties of kaolin as raw material, the physical properties of metakaolin, and the functional groups of kaolin and metakaolin were evaluated in the first phase of this study. The mortar produced consisted of 65% fine aggregate and 35% paste, while the pasta contained 60% metakaolin and 40% alkaline solution. The specimens are listed in Table 1 with a 0%, 0.5%, 1%, 1.5%, and 2% variation of the weight of the raw material of bemban fiber. MbG_F0 indicates 100% metakaolin as raw material with 0% bemban fiber, while MbG_F0.5 denotes 0.5% bemban fiber. An hour prior to casting, sodium hydroxide and sodium silicate were mixed. The raw material was progressively combined with the alkali activator, and the combination was stirred for 2 min to form a paste in the mixer. After that, the fine aggregate was poured into the fresh geopolymer paste to form a geopolymer mortar mixture. Last, the bemban fiber was inserted into the mortar to form metakaolin-based geopolymer mortar. The constituent material of metakaolin-based geopolymers using bemban fiber is depicted in Figure 1.

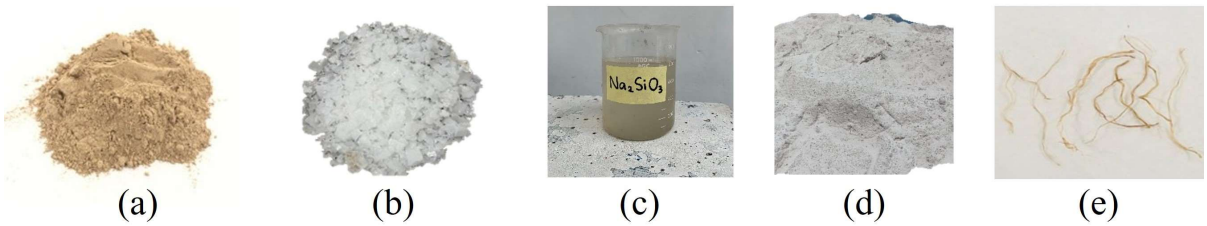

Figure 1. The constituent materials of metakaolin-based geopolymer using bemban fiber mortar. (a) Metakaolin, (b) NaOH, (c) Na_2SiO_3, (d) silica sand and (e) bemban fiber.

The fresh geopolymer mortar was then cast in a 38 mm diameter cylinder with a height of 76 mm. The mortar mold was opened after 24 h and cured at a humid temperature using a moist towel for 28 days until the days of testing, as seen in Figure 2.

The physical assessments, including porosity and water absorption, compressive strength based on ASTM C39, and splitting tensile strength according to ASTM C496/C496M, were investigated in the second phase of research. Further, the details of the mix proportion of metakaolin-based geopolymer with additive bemban fiber are shown in Table 2.

Figure 2. Metakaolin-based geopolymer using bemban fiber mortar. (a) specimen and (b) curing procedure.

Table 1. Composition of metakaolin-based geopolymer specimens.

Code	Metakaolin (%)	Bemban fiber (%)
MbG-F0	100	0
MbG-F0.5	100	0.5
MbG-F1.0	100	1.0
MbG-F1.5	100	1.5
MbG-F2.0	100	2.0

Table 2. Details of mix proportion.

Code	Kaolin (g)	NaOH (g)	Na_2SiO_3 (mL)	Fine aggregate (g)	Bemban fiber (g)
MbG-F0	214.92	72	180	665.24	0.00
MbG-F0.5	214.92	72	180	665.24	1.07
MbG-F1.0	214.92	72	180	665.24	2.15
MbG-F1.5	214.92	72	180	665.24	3.22
MbG-F2.0	214.92	72	180	665.24	4.30

3. Results and discussion

3.1. Chemical composition

The composition of oxide compounds in kaolin as a geopolymer base material using XRF is shown in Table 3. It can be observed that kaolin consists of 59.30% SiO_2, 34.30% Al_2O_3, and 3.06% Fe_2O_3. From this data, it is evident that the kaolin used has a high content of SiO_2 and Al_2O_3, which are beneficial in producing geopolymers.

Table 3. Chemical composition of kaolin from Kupang Mountain.

Chemical composition	Percentage (%)	Chemical composition	Percentage (%)
SiO_2	59.30	NiO	0.08
Al_2O_3	34.30	MnO	0.05
Fe_2O_3	3.06	Re_2O_7	0.05
K_2O	1.27	CuO	0.04
P_2O_5	0.70	Cr_2O_3	0.04
TiO_2	0.66	V_2O_5	0.03
CaO	0.29	Yb_2O_3	0.02
Eu_2O_3	0.08	ZnO	0.00

The content of other elements is too small to significantly affect the manufacture of geopolymers. In making geopolymers, the SiO_2 and Al_2O_3 content in kaolin reacts with alkaline solutions to form silicate and alumino-silicate polymer chains, providing strength and stiffness to the geopolymer material. In line with Giese's [31] statement, the silicate in kaolin functions as the main component of inorganic polymers, while alumina provides special properties such as hardness, strength, and refractoriness.

Hasfianti [17] analyzed Tatakan (Rantau) kaolin with XRF and found a low-value content, namely, SiO_2 at 55.92% and Al_2O_3 at 29.13%. Limamar (Martapura) kaolin had a composition of SiO_2 (55.04%) and Al_2O_3 (32.71%), and imported Taiwanese kaolin with SiO_2 (54.63%) and Al_2O_3 (28.23%). This shows that Mount Kupang (Banjarbaru) kaolin contains a higher amount of SiO_2 and Al_2O_3 than kaolin from other areas of South Kalimantan, indicating its great potential as a material for geopolymers.

3.2. Thermal properties of kaolin

Kaolin, applied as a geopolymer material, is hydroxylated to become metakaolin. The transformation of kaolin into metakaolin with temperature and holding time was determined through thermal stability tests and analyzed using TGA and DTA. Several processes are explained in the TGA-DTA kaolin curve shown in Figure 3. Thermal events occur in kaolin during the heating process at temperatures from 30 to 900 °C, namely predehydroxylation, dehydroxylation, and endothermy. The predehydroxylation event occurs at a temperature of 31.07–92.69 °C, possibly due to the evolution of small amounts of water, followed by a mass reduction of 1.3% [27]. Dehydroxylation events occur in the range of 400–600 °C, usually involving the dehydroxylation of the mineral kaolinite [32]. The endothermic peak in the DTA curve (blue line) was recorded at a temperature of 505.63 °C, where the sample absorbed heat from the environment, followed by a mass reduction of up to 9.4%. In this situation,

kaolin experienced a loss of the OH lattice in water, indicating the proper occurrence of the dehydroxylation process [27]. The reactions occurring in this event are shown in Eq 1 based on the research of Longhi et al. [33].

$$Al_2O_3 \cdot 2SiO_2 \cdot 2H_2O(s) \rightarrow Al_2O_3 \cdot 2SiO_2(s) + 2H_2O(g) \quad (1)$$

Kaolin Metakaolin Water

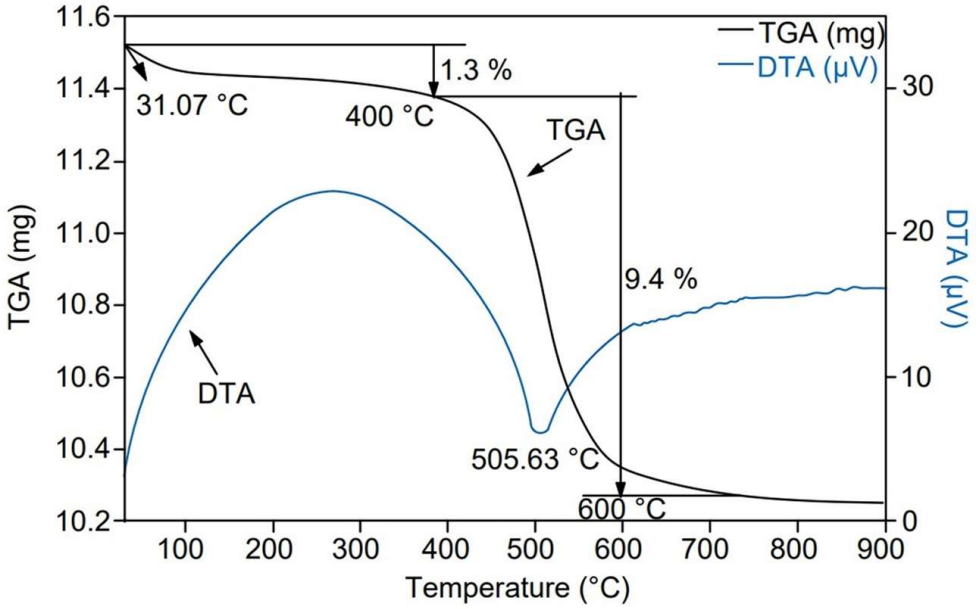

Figure 3. DTA-TGA kaolin curve.

The dehydroxylation event results in a change in the crystalline phase of kaolin ($SiO_2 \cdot 2Al_2O_3 \cdot 2H_2O$) to amorphous metakaolin ($SiO_2 \cdot 2Al_2O_3$) [27]. It becomes reactive when activated with NaOH and Na_2SiO_3 activators for geopolymer applications. The results of the TGA-DTA thermal analysis are then used to determine the calcination temperature by examining the absorption peaks in the FTIR spectral pattern.

3.3. Physical properties of metakaolin

Testing of physical properties is shown in Table 4. Notably, the water content of metakaolin is quite low due to heating by calcination, which is also confirmed by the results of the chemical bond and functional group testing using FTIR in Figure 4. Table 4 describes the water content, density, and porosity of metakaolin powder that has passed through a 200-mesh sieve. The testing procedure was based on SNI 8460:2017 [34]. The water content of metakaolin with calcination is also influenced by the temperature and time of calcination, as reported by Khaled et al. [23].

Table 4. Physical properties of metakaolin.

Physical properties	Value
Water content (%)	0.12 ± 0.02
Density (g/cm^3)	2.22 ± 0.00
Porosity (%)	31.14 ± 0.06

The calcination process can cause the release of water molecules in kaolin due to the dehydration process. The water content in metakaolin can also affect the porosity of the geopolymer, with high water content tending to produce geopolymers with higher porosity, as excess water can leave empty spaces in the geopolymer structure after the manufacturing process. Low water content can produce geopolymers with smaller porosity [35]. The water content of metakaolin in this study was lower than that of Tatakan and Limamar, with values of 3.60% and 4.75%, respectively [17]. It can be concluded that metakaolin with low water content can be used as a geopolymer base material. In this study, calcination of kaolin was carried out at a temperature of 600 °C, based on the results of the stability test of its thermal properties using DTA and TGA (Figure 4).

The density of metakaolin is shown in Table 4, with a value of 2.22 g/cm^3. Metakaolin density can affect the mechanical strength of geopolymers—the higher the metakaolin density, the more likely it is to produce a geopolymer with higher mechanical strength. A high density indicates denser metakaolin particles, which can result in stronger bonding and filling [36]. In this study, metakaolin density was higher than in the research by Oliveira et al. [37], which obtained a metakaolin density of 1.57 g/cm^3.

Density and porosity have an inverse relationship in the context of certain materials or substances. Generally, the higher the density of a material, the lower the porosity, and vice versa [38]. Metakaolin porosity is shown in Table 4 with a value of 31.14%. The metakaolin porosity in this study was lower than in the research by Sinngu et al. [39], which obtained a metakaolin porosity of 47.23%. The physical characteristics of metakaolin can provide information for its application as a geopolymer base material.

3.4. Functional groups of kaolin and metakaolin

Identification of functional groups in kaolin and metakaolin was carried out using FTIR with a wave number range of 4000–500 cm^{-1}. Figure 4 shows the FTIR spectra of kaolin and metakaolin. There are differences in the absorption peaks and wave numbers obtained, indicating the functional groups and bonds formed in kaolin after it becomes metakaolin.

The Infrared Radiation (IR) spectra of kaolin before and after calcination at various temperatures and holding times of 2 h are shown in Figure 4. Kaolin before calcination has a typical absorption peak at a wave number of 3689 cm^{-1}, which is the stretching vibration of the O–H group of the octahedral surface forming weak hydrogen bonds with oxygen from Si–O–Si bonds in the next layer, resulting in stretching bands [36]. The 3618 cm^{-1} peak is related to O–H stretching vibrations caused by the inner hydroxyl groups located between the tetrahedral and octahedral sheets [40]. The 1634 cm^{-1} band associated with O–H bending vibrations indicates the presence of water molecules [41]. The absorption bands at 1114, 1025, and 1003 cm^{-1} related to Si–O stretching bands are characteristic of clays with trivalent atoms in octahedral sheets, which are possessed only by kaolinite [23,27,35,42]. The 909 cm^{-1}

shows O–H bending, indicating that kaolinite has a trivalent central atom in an octahedral sheet [41]. The 788 and 749 cm^{-1} bands are related to O–H bending bands, where most of them have Al (III) in the octahedral position, which forms Al–OH [35,36]. Absorption bands at 682 and 640 cm^{-1} are where most of the octahedral sites are occupied by divalent central atoms [40]. In places where clay has most of its octahedral sites occupied by divalent central atoms such as Mg(II) or Fe(II), O–H stretching areas are often found [43]. The absorption band at 527 cm^{-1} shows the stretching vibration absorption of Si–O–Al (IV) where, at that time, Al was in an octahedral coordination state.

The calcination process causes kaolin to lose its characteristic peaks at wave numbers 3689, 3618, and 1634 cm^{-1}. This phenomenon shows that temperature variations can transform kaolin into metakaolin. Additionally, the absorption band found in kaolin before calcination at the wave number of 1025 cm^{-1} has shifted to wave numbers 1035, 1040, 1051, 1043, 1045, and 1048 cm^{-1}, which is the absorption region for amorphous SiO_2 [42]. Absorption in the 700 and 600 cm^{-1} area show that the presence of alumina components and other dominating components such as Fe persists. These results agree with the research conducted by [27,28,44].

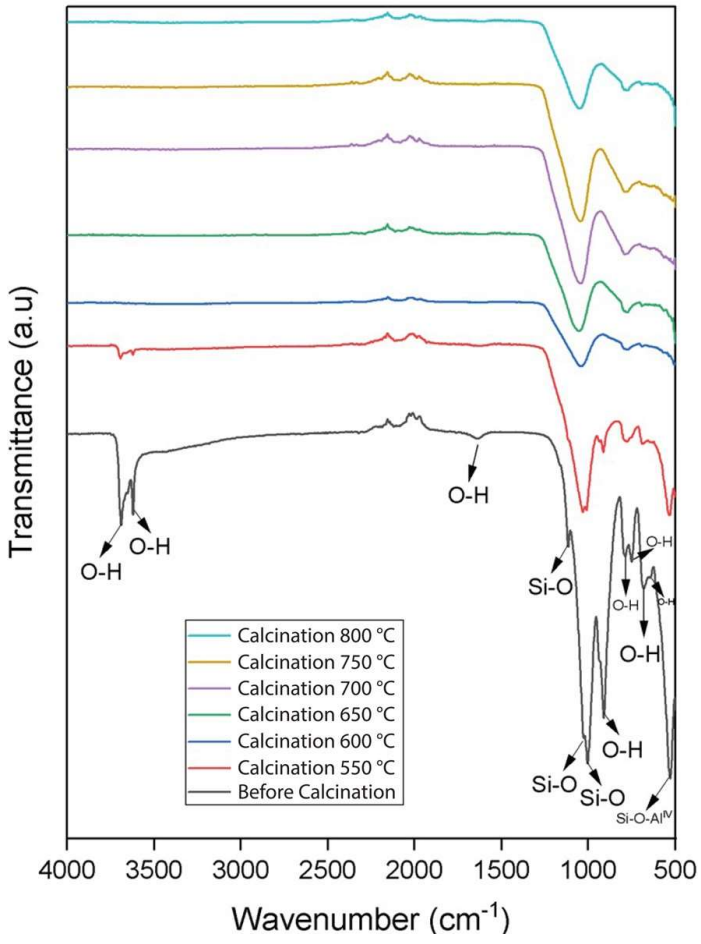

Figure 4. FTIR spectra of kaolin and metakaolin.

Similarities can be observed in the FTIR spectral patterns of all heat treatments based on the wave number. However, differences appear only in the transmittance intensity of each sample. The temperature variations in this study were 550, 600, 650, 700, 750, and 800 °C for 2 h. The wave number

shift in the FTIR spectra shows a gentle decrease in the curve at a temperature of 600 °C compared to other calcination variations. At 600 °C, with a calcination time of 2 h, there is a decrease in dip, which increasingly becomes a flat shape with a lower FTIR dip shape, compared to the others. According to Erasmus [45], this indicates an increase in amorphous formation before finally transforming into another phase in crystalline form. This is also confirmed by Tironi et al. [46]. Based on the FTIR results, it can be concluded that the optimum calcination temperature and holding time for Mount Kupang natural kaolin is 600 °C, with a holding time of 2 h.

Various studies have been carried out on the calcination of kaolin to become metakaolin with varying temperatures and holding times, including at 700 °C for 30 min [36], 800 °C for 6 h [47], and 750 °C for 3 h [27], with various kaolin sources. This research was carried out with variations of 550, 600, 650, 700, 750, and 800 °C for 2 h, which is a novelty in the kaolin calcination of Mount Kupang. It can be concluded that calcination at 600 °C for 2 h is the optimum condition for kaolin originating from Mount Kupang, Banjarbaru.

3.5. Characteristic metakaolin-based geopolymer with the addition of bemban fiber

Testing for water absorption refers to SNI 03-0349-1989. The physical properties test was conducted to determine the percentage of water absorbed by each sample. The water absorption and porosity of geopolymers are shown in Table 5 and Figure 5, evidencing a range from 1.10% to 4.44%. Differences in water absorption for all samples are evident, with the MbG-F1.5 sample having relatively lower water absorption. The difference in the water absorption value of geopolymers is due to the composition of the constituent material, namely kaolin, which is related to the adhesion between matrices influenced by the physical and chemical characteristics of the material. Table 5 shows that the water absorption value decreases as the use of bemban fiber increases, with the lowest value in geopolymers with 1.5% bemban fiber, which is the optimum level. It then increases again, possibly due to an excess of fibers causing cavities. Further, the alkalization of bemban fiber can reduce water absorption and make the specimen hydrophobic, thereby increasing density and lowering porosity.

Table 5. Physical characteristics of metakaolin-based geopolymer.

Code	Water absorption (%)	Porosity (%)
MbG-F0	4.44	9.29
MbG-F0.5	3.33	6.96
MbG-F1.0	2.76	5.80
MbG-F1.5	1.10	2.32
MbG-F2.0	2.20	4.64

The geopolymer porosity values are shown in Table 5, ranging between 2.32% and 9.29%, with an average porosity of 5.80%. It can be observed that porosity decreases with increasing percentages of bemban fiber, with 1.5% bemban fiber being the optimum level of use. It then increases again, possibly due to an excess of fibers causing cavities. The low porosity value with the addition of bemban fiber is due to the alkalization treatment, which can reduce fiber porosity and increase the adhesive properties between fiber and matrix. The highest porosity is 9.29% in the MbG-F0 specimen and the lowest is 2.32% in MbG-F1.5.

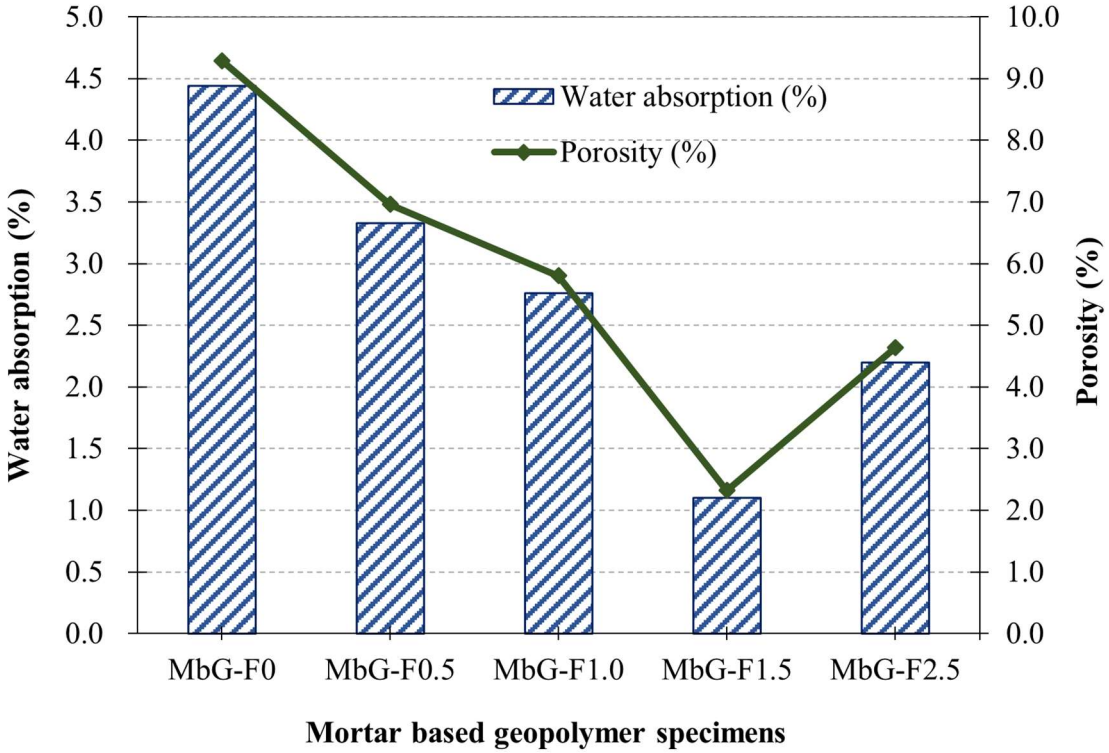

Figure 5. Relationship between water absorption and porosity of specimens.

The porosity value in this study is lower than in the research by Walbrück et al. [48], which used natural fibers to obtain a porosity of 49%–76%. Yanou et al. [49], using 1.5% sugarcane bagasse fiber, obtained a geopolymer porosity of 12%. It can be concluded that porosity is closely related to compressive strength.

3.6. Compressive strength

There are differences in compressive strength based on each composition and with the addition of bemban fibers, as shown in Table 6 and Figure 6. In geopolymers, the SiO_2 and Al_2O_3 content in kaolin reacts with the activator solution to form silicate and alumino-silicate polymer chains, providing strength and stiffness. In line with Giese Jr.'s statement [31], the silicate in the geopolymer material serves as the main component of inorganic polymers, providing hardness and strength properties, while alumina provides special properties such as refractoriness.

Table 6. Compressive strength of metakaolin-based geopolymer.

Code	Maximum load (N)	Compressive strength (MPa)	Splitting test strength (MPa)
MbG-F0	24570.56	22.11	7.28
MbG-F0.5	32401.17	29.15	9.48
MbG-F1.0	37152.49	33.43	10.52
MbG-F1.5	39270.73	35.33	11.29
MbG-F2.0	32680.66	29.40	9.26

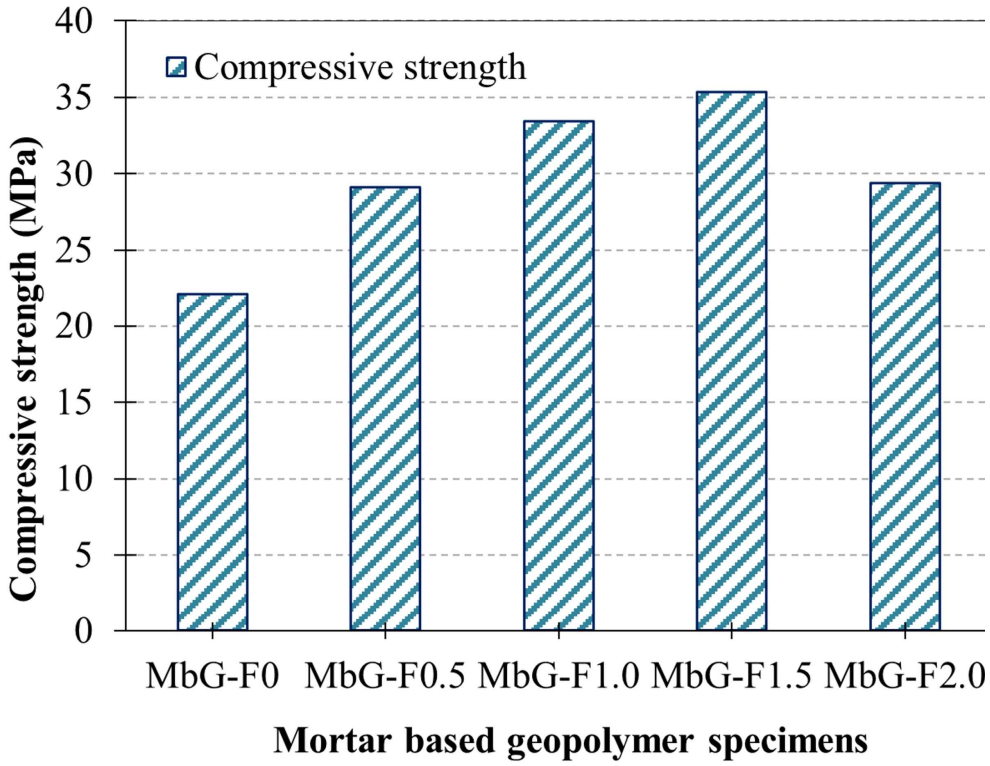

Figure 6. Compressive strength of metakaolin-based geopolymers with fiber content.

Additionally, the heating or calcination process of kaolin can transform into metakaolin, as shown in Figure 3, making it reactive to the NaOH activator solution. The compressive strength of the geopolymer in this study is higher than in the research by Cai et al. [50], which provided a compressive strength of 16.23–21.94 MPa, and by Ayeni et al. [51], which obtained a compressive strength of 4.49–5.56 MPa. Further, the addition of 0.5–2% bemban fiber can also increase the compressive strength of the geopolymer, as shown in Table 6.

3.7. Splitting tensile strength

As summarized in Table 6 dan Figure 7, bemban fiber has a significant effect on the splitting test of specimens. With the increasing percentage of bemban fiber in the mixture, the splitting tensile test of metakaolin-based geopolymer specimens improved. In line with the compressive strength result, the optimum percentage of bemban fiber is 1.5% by weight of raw material in the mixture. The highest splitting tensile strength was in MbG-F1.5 at 11.29 MPa.

Anwar and Ella [52] found that adding fibers to geopolymers can increase their mechanical strength by 30%–70%. However, when the fiber reaches the optimum limit, a decrease will occur. The values of splitting tensile strength with bemban fiber at 0.5%, 1.0%, 1.5%, 2.0%, and 2.5% are, respectively, 23.21%, 30.80%, 35.52%, and 21.38% higher than that with metakaolin-based geopolymer specimens without bemban fiber. The addition of fibers greater than 1.5% results in a decrease in the compressive strength and splitting tensile strength of the geopolymer test sample, caused by excessive fiber filling the test sample, resulting in spaces between the geopolymer matrix, which is related to the geopolymer porosity shown in Table 5. This aligns with previous research that

concluded that the addition of fiber can strengthen the geopolymer; however, when the amount exceeds the optimum level, the compressive strength will decrease because the fiber will create more space between the geopolymer matrix [53,54].

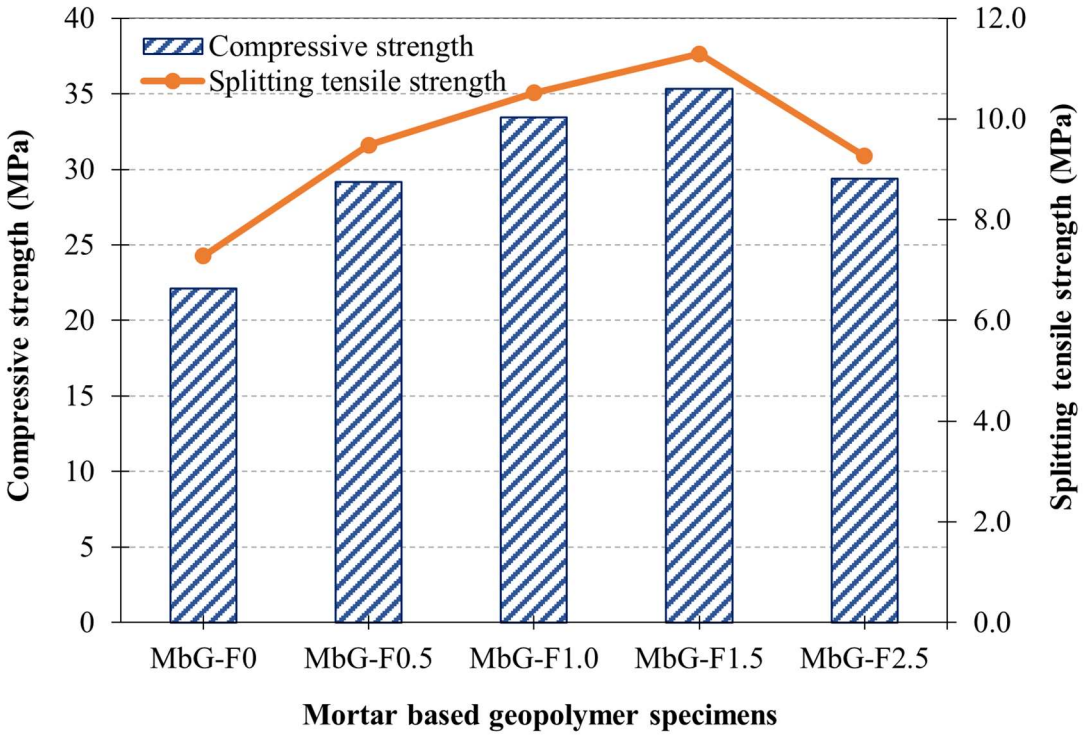

Figure 7. Relationship between splitting tensile strength and compressive strength.

The splitting tensile strength test results strengthen the conclusion regarding the percentage of bemban fiber [34]. Experimental results found that the highest splitting tensile strength was in MbG-F1.5 geopolymer at 11.29 MPa, with the addition of 1.5% bemban fiber. Although the split tensile strength increases as the fiber content increases, 1.5% is the optimum because higher values decrease the workability of mixtures.

4. Conclusions

The aim of this study is to investigate the physical and mechanical properties of metakaolin-based geopolymers using bemban fiber additives. The results are summarized as follows:

1. Kaolin chemical composition consists of 59.30% SiO_2, 34.30% Al_2O_3, and 3.06% Fe_2O_3.
2. To convert kaolin into metakaolin, optimum calcination process conditions are 600 °C for 2 h.
3. Thermal properties of kaolin, such as predehydroxylation, occur at 31.07–92.69 °C; dihydroxylation occurs in the range of 400–600 °C; the endothermic peak in the DTA curve is recorded at a temperature of 505.63 °C.
4. Adding 1.5% bemban fiber to the metakaolin-based geopolymer can improve its physical properties by reducing the percentage of water absorption to 1.10% and porosity to 2.32% while increasing the compressive strength and splitting tensile strength to 35.33 and 11.29 MPa, respectively.

5. One strategy to enhance geopolymers' tensile strength and flexibility is by adding natural fibers. Further research is needed to assess the resistance of fiber-reinforced geopolymers in aggressive environments, such as acidic and salty coastal environments, for application in industries focusing on sustainable construction.

Use of AI tools declaration

The authors declare they have not used Artificial Intelligence (AI) tools in the creation of this article.

Acknowledgments

This study was supported by the DRTPM Grant Program under contract numbers 056/E5/PG.02.00.PL/2024 and 1043/UN8.2/PG/2024, funded by the Indonesian Ministry of Education, Culture, Research, and Technology.

Author contributions

Nursiah Chairunnisa: writing–review & editing, supervision, methodology, conceptualization; Ninis Hadi Haryanti: writing–review & editing, original draft, validation, investigation, conceptualization; Ratni Nurwidayati: writing–review & editing, methodology, data curation; Ade Yuniati Pratiwi: writing–review & editing, methodology, data curation; Yudhi Arnandha: writing–review & editing, methodology, data curation; Tetti N Manik: writing – review & editing, methodology, data curation; Suryajaya: writing–review & editing, methodology, data curation; Yoga Saputra: investigation, data curation; Nur Hazizah: investigation, data curation.

Conflict of interest

The authors declare no conflict of interest.

References

1. Choi YC (2022) Hydration and internal curing properties of plant-based natural fiber-reinforced cement composites. *Case Stud Constr Mater* 17: e01690. https://doi.org/10.1016/j.cscm.2022.e01690
2. Camargo MM, Taye EA, Roether JA, et al. (2020) A review on natural fiber-reinforced geopolymer and cement-based composites. *Materials (Basel)* 13: 4603. https://doi.org/10.3390/ma13204603
3. Alsalman A, Assi LN, Kareem RS, et al. (2021) Energy and CO_2 emission assessments of alkali-activated concrete and ordinary Portland cement concrete: A comparative analysis of different grades of concrete. *Clean Environ Syst* 3: 100047. https://doi.org/10.1016/j.cesys.2021.100047
4. Turner LK, Collins FG (2013) Carbon dioxide equivalent (CO_{2-e}) emissions: A comparison between geopolymer and OPC cement concrete. *Constr Build Mater* 43: 125–130. http://dx.doi.org/10.1016/j.conbuildmat.2013.01.023

5. Huntzinger DN, Eatmon TD (2009) A life-cycle assessment of Portland cement manufacturing: Comparing the traditional process with alternative technologies. *J Clean Prod* 17: 668–675. https://doi.org/10.1016/j.jclepro.2008.04.007
6. Soutsos M, Boyle AP, Vinai R, et al. (2016) Factors influencing the compressive strength of fly ash based geopolymers. *Constr Build Mater* 110: 355–368. http://dx.doi.org/10.1016/j.conbuildmat.2015.11.045
7. Xue C, Sirivivatnanon V, Nezhad A, et al. (2023) Comparisons of alkali-activated binder concrete (ABC) with OPC concrete—A review. *Cem Concr Compos* 135: 104851. https://doi.org/10.1016/j.cemconcomp.2022.104851
8. Rashad AM, Zeedan SR (2011) The effect of activator concentration on the residual strength of alkali-activated fly ash pastes subjected to thermal load. *Constr Build Mater* 25: 3098–3107. http://dx.doi.org/10.1016/j.conbuildmat.2010.12.044
9. Verma M, Chouksey A, Meena RK, et al. (2023) Analysis of the properties of recycled aggregates concrete with lime and metakaolin. *Mater Res Express* 10: 095508. https://doi.org/10.1088/2053-1591/acf983
10. Okoye FN, Prakash S, Singh NB (2017) Durability of fly ash based geopolymer concrete in the presence of silica fume. *J Clean Prod* 149: 1062–1067. https://doi.org/10.1016/j.jclepro.2017.02.176
11. Huseien GF, Sam ARM, Shah KW, et al. (2019) Evaluation of alkali-activated mortars containing high volume waste ceramic powder and fly ash replacing GBFS. *Constr Build Mater* 210: 78–92. https://doi.org/10.1016/j.conbuildmat.2019.03.194
12. Timakul P, Rattanaprasit W, Aungkavattana P (2016) Enhancement of compressive strength and thermal shock resistance of fly ash-based geopolymer composites. *Constr Build Mater* 121: 653–658. http://dx.doi.org/10.1016/j.conbuildmat.2016.06.037
13. Sá Ribeiro RA, Sá Ribeiro MG, Sankar K, et al. (2016) Geopolymer-bamboo composite—A novel sustainable construction material. *Constr Build Mater* 123: 501–507. https://doi.org/10.1016/j.conbuildmat.2016.07.037
14. Rumbayan R, Sudarno S (2020) Kuat tekan , kuat lentur dan daya serap air untuk batako dengan penambahan serat sabut kelapa. *J Polimdo* 2: 145–153. http://dx.doi.org/10.47600/jtst.v2i3.255
15. Syarief A, Basyir AA, Nugraha A (2021) Pengaruh orientasi serat dan waktu alkalisasi pada laminates composite polyester-serat bemban (donax canniformis) terhadap kekuatan bending, impact dan bentuk patahan. *Info-Teknik* 22: 209. https://doi.org/10.20527/infotek.v22i2.12387
16. Alviyanda A, Sipayung CS (2023) Studi batuan asal (provenance) batupasir formasi simpangaur daerah way krui Lampung. *J Sci Appl Technol* 7: 26–34. https://journal.itera.ac.id/index.php/jsat/article/view/1086
17. Hasfianti FE, Prabawa IGDP, Nurhidayati N, et al. (2021) Potensi pemanfaatan kaolin asal kalimantan selatan sebagai pengganti clay impor pada pembuatan papan semen. *J Keramik dan Gelas Indones* 30. Available from: https://media.neliti.com/media/publications/453234-potential-utilization-of-kaolin-from-sou-3e5f8942.pdf.
18. Sarah KMAS, Géber R, Simon A, et al. (2023) Comparative study of metakaolin-based geopolymer characteristics utilizing different dosages of water glass in the activator solution. *Results Eng* 20: 101469. https://doi.org/10.1016/j.rineng.2023.101469

19. Sá Ribeiro RA, Sá Ribeiro MG, Kriven WM (2017) A review of particle- and fiber-reinforced metakaolin-based geopolymer composites. *J Ceram Sci Technol* 8: 307–322. https://doi.org/10.4416/JCST2017-00048
20. Mohamed OA, Al Khattab R (2022) Fresh properties and sulfuric acid resistance of sustainable mortar using alkali-activated GGBS/fly ash binder. *Polymers (Basel)* 14: 591. https://doi.org/10.3390/polym14030591
21. Mohamed OA (2023) Effects of the curing regime, acid exposure, alkaline activator dosage, and precursor content on the strength development of mortar with alkali-activated slag and fly ash binder: a critical review. *Polymers (Basel)* 15: 1248. https://doi.org/10.3390/polym15051248
22. Kaya M, Köksal F, Bayram M, et al. (2023) The effect of marble powder on physico-mechanical and microstructural properties of kaolin-based geopolymer pastes. *Struct Concr* 24: 6485–6504. https://doi.org/10.1002/suco.202201010
23. Khaled Z, Mohsen A, Soltan AM, et al. (2023) Optimization of kaolin into Metakaolin: Calcination conditions, mix design and curing temperature to develop alkali activated binder. *Ain Shams Eng J* 14: 102142. https://doi.org/10.1016/j.asej.2023.102142
24. Jindal BB, Alomayri T, Hasan A, et al. (2023) Geopolymer concrete with metakaolin for sustainability: a comprehensive review on raw material's properties, synthesis, performance, and potential application. *Environ Sci Pollut Res* 30: 25299–25324. https://doi.org/10.1007/s11356-021-17849-w
25. Van Deventer JSJ, Provis JL, Duxson P (2012) Technical and commercial progress in the adoption of geopolymer cement. *Miner Eng* 29: 89–104. http://dx.doi.org/10.1016/j.mineng.2011.09.009
26. Zhang ZH, Zhu HJ, Zhou CH, et al. (2016) Geopolymer from kaolin in China: An overview. *Appl Clay Sci* 119: 31–41. http://dx.doi.org/10.1016/j.clay.2015.04.023
27. Saukani M, Sholehah I, Arief S, et al. (2020) Karakterisasi stabilitas termal kaolin tatakan Kalimantan Selatan. *J Fis dan Apl* 16: 29–32. https://doi.org/10.12962/j24604682.v16i1.4756
28. Cong PL, Cheng YQ (2021) Advances in geopolymer materials: A comprehensive review. *J Traffic Transp Eng (English Ed)* 8: 283–314. https://doi.org/10.1016/j.jtte.2021.03.004
29. Abdalla JA, Hawileh RA, Bahurudeen A, et al. (2023) A comprehensive review on the use of natural fibers in cement/geopolymer concrete: A step towards sustainability. *Case Stud Constr Mater* 19: e02244. https://doi.org/10.1016/j.cscm.2023.e02244
30. Shilar FA, Ganachari SV, Patil VB, et al. (2022) Evaluation of structural performances of metakaolin based geopolymer concrete. *J Mater Res Technol* 20: 3208–3228. https://doi.org/10.1016/j.jmrt.2022.08.020
31. Giese Jr. RF (2018) Kaolin minerals: Structures and stabilities, In: Bailey SW, *Hydrous Phyllosilicates*, Berlin: De Gruyter, 29–66.
32. Faqir NM, Shawabkeh R, Al-Harthi M, et al. (2019) Fabrication of geopolymers from untreated kaolin clay for construction purposes. *Geotech Geol Eng* 37: 129–137. https://doi.org/10.1007/s10706-018-0597-5
33. Longhi MA, Rodríguez ED, Bernal SA, et al. (2016) Valorisation of a kaolin mining waste for the production of geopolymers. *J Clean Prod* 115: 265–272. https://doi.org/10.1016/j.jclepro.2015.12.011
34. Badan Standardisasi Nasional (2017) Persyaratan perancangan geoteknik. *Standar Nas Indones* 8460.

35. Méité N, Konan LK, Tognonvi MT, et al. (2022) Effect of metakaolin content on mechanical and water barrier properties of cassava starch films. *South African J Chem Eng* 40: 186 https://doi.org/10.1016/j.sajce.2022.03.005
36. Kenne Diffo BB, Elimbi A, Cyr M, et al. (2015) Effect of the rate of calcination of kaolin on the properties of metakaolin-based geopolymers. *J Asian Ceram Soc* 3: 130–138. http://dx.doi.org/10.1016/j.jascer.2014.12.003
37. Oliveira LB, Marvila MT, Fediuk R, et al. (2023) Development of a complementary precursor based on flue gas desulfurization (FGD) for geopolymeric pastes produced with metakaolin. *J Mater Res Technol* 22: 3489–3501. https://doi.org/10.1016/j.jmrt.2023.01.017
38. Zunino F, Scrivener K (2021) The reaction between metakaolin and limestone and its effect in porosity refinement and mechanical properties. *Cem Concr Res* 140: 106307. https://doi.org/10.1016/j.cemconres.2020.106307
39. Sinngu F, Ekolu SO, Naghizadeh A, et al. (2023) Evaluation of metakaolin pozzolan for cement in South Africa. *Dev Built Environ* 14: 100154. https://doi.org/10.1016/j.dibe.2023.100154
40. Ulfiati R, Dhaneswara D, Fatriansyah JF, et al. (2020) The effect of calcination temperature on metakaolin characteristic synthesized from badau belitung kaolin. *Key Eng Mater* 841: 312–316. https://doi.org/10.4028/www.scientific.net/KEM.841.312
41. Purbasari A, Samadhi TW (2021) Kajian dehidroksilasi termal kaolin menjadi metakaolin menggunakan analisis termogravimetri. *Alchemy J Penelit Kim* 17: 105–112. https://doi.org/10.20961/alchemy.17.1.47337.105-112
42. Liew YM, Kamarudin H, Mustafa Al Bakri AM, et al. (2012) Processing and characterization of calcined kaolin cement powder. *Constr Build Mater* 30: 794–802. https://doi.org/10.1016/j.conbuildmat.2011.12.079
43. Stuart BH (2004) *Infrared Spectroscopy: Fundamentals and Applications*, New York: John Wiley & Sons.
44. Essaidi N, Samet B, Baklouti S, et al. (2014) Feasibility of producing geopolymers from two different Tunisian clays before and after calcination at various temperatures. *Appl Clay Sci* 88–89: 221–227. http://dx.doi.org/10.1016/j.clay.2013.12.006
45. Erasmus E (2016) The influence of thermal treatment on properties of kaolin. *Hem Ind* 70: 66–66. https://doi.org/10.2298/HEMIND150720066E
46. Tironi A, Trezza MA, Irassar EF, et al. (2012) Thermal treatment of kaolin: Effect on the pozzolanic activity. *Procedia Mater Sci* 1: 343–350. https://doi.org/10.1016/j.mspro.2012.06.046
47. Paulus JM, Supit S, Mantiri H (2022) Karakteristik mekanik campuran panel dinding berbahan dasar metakaolin dan serat bambu. *J Tek Sipil Terap* 4: 1–10. https://doi.org/10.47600/jtst.v4i1.364
48. Walbrück K, Drewler L, Witzleben S, et al. (2021) Factors influencing thermal conductivity and compressive strength of natural fiber-reinforced geopolymer foams. *Open Ceram* 5: 100065. https://doi.org/10.1016/j.oceram.2021.100065
49. Yanou RN, Kaze RC, Adesina A, et al. (2021) Performance of laterite-based geopolymers reinforced with sugarcane bagasse fibers. *Case Stud Constr Mater* 15: e00762. https://doi.org/10.1016/j.cscm.2021.e00762
50. Cai JM, Li XP, Tan JW, et al. (2020) Thermal and compressive behaviors of fly ash and metakaolin-based geopolymer. *J Build Eng* 30: 101307. https://doi.org/10.1016/j.jobe.2020.101307

51. Ayeni O, Onwualu AP, Boakye E (2021) Characterization and mechanical performance of metakaolin-based geopolymer for sustainable building applications. *Constr Build Mater* 272: 121938. https://doi.org/10.1016/j.conbuildmat.2020.121938
52. Anwar S, Kusumastuti E (2016) Pemanfaatan serat pohon pisang dalam sintesis geopolimer abu layang batubara. *Indo J Chem Sci* 5. https://doi.org/10.15294/ijcs.v5i1.9170
53. Mariamah, Chairunnisa N, Nurwidayati R (2023) The effect of natrium hydroxide molarity variation and alkali ratio on the compressive strength of geopolymer paste and mortar. *IOP Conf Ser Earth Environ Sci* 1184: 012025. https://doi.org/10.1088/1755-1315/1184/1/012025
54. Haryanti NH, Chairunnisa N, Nurwidayati R, et al. (2023) The potential of bemban fiber as raw material of geopolymer. *Int J Geomate* 25: 21–31. https://doi.org/10.21660/2023.112.4083